

## Air Impingement Drying of Foods: Modelling Coupled Heat and Mass Transfer and Experimental Validation

Tidjani Bahar, Virginie Boy, Yves Lemée, Anthony Magueresse, Thomas Lendormi\*, Patrick Glouannec, Jean-Louis Lanoisellé

Univ. Bretagne Sud, UMR CNRS 6027, IRDL, F-56300 Pontivy, France  
 thomas.lendormi@univ-ubs.fr

A numerical model was developed to predict heat and mass transfers within the product and the boundaries conditions of temperature and airflow around the product during the drying of infinite slabs. Variable thermophysical and hygric properties during the drying were also included in the model. Effective moisture diffusivity was a function of the temperature. Convective coefficient was estimated by a direct measurement using a fluxmeter. A system of non-linear unsteady-state partial differential equations were solved by using finite elements methods. Air impingement drying of a gel made of carboxymethylcellulose (CMC) to simulate water-rich foods from 40 °C to 70 °C and from 1 m s<sup>-1</sup> to 17 m s<sup>-1</sup> was studied. Predicted results were found fairly well in line with the experimental ones ( $R^2 = 0.994$ ,  $\chi^2 = 4.758 \cdot 10^{-4}$ ,  $RMSE = 0.021$  and  $RSS = 0.009$ ).

### 1. Introduction

Thermal drying of foods is still a major challenge because foods are heat sensitive and it is needed to optimize the energy consumption of the process. Several numerical models were developed to describe the drying kinetics of food products often specific to a particular type of product and to the process conditions. For instance, Cascone et al. (2015) developed a numerical model able to describe the irregular shape and the volume shrinking during the drying process of an Italian sausage. Reyes et al. (2015) studied the influence of onion thickness using a hybrid solar dryer, a tunnel dryer and a freeze-dryer. The many studies devoted to the drying process of food products demonstrate that broad-based and adaptable models should be developed (Cursio et al., 2008).

Impinging jets are largely employed to increase the performances of industrial dryers (Mujumdar, 2006). Numerous investigations have demonstrated the benefits of impingement jets in heat transfer applications, including drying. The application of air impingement jets is mostly used to increase the heat transfer coefficient and thus to reduce the drying time. However, the use of most of the drying models to predict the performances of air impingement jets dryers is no longer possible due to the complexity of boundaries conditions (fluid dynamics).

The Tylose® gel was chosen as a model food. This product was traditionally used to study the heat transfer in freezing processes. Hence, Tylose® properties (effective moisture diffusivity, thermophysical and hygric properties) are available in the literature for a temperature range from -10 °C to 40 °C. The main novelty of this work is to investigate the drying process of the Tylose® gel and to characterize its properties between 40 °C and 70 °C. Moreover, these research works are intended to develop a numerical mathematical model in order to predict heat and mass transfers within the product and the boundaries conditions of temperature and airflow around the product during the drying of infinite slabs.

The developed model will take into account the influence of the water activity on the mass transfer at the interface air/product. Variable Tylose® gel properties as a function of temperature and/or moisture content will be also considered. A constant heat transfer coefficient will be incorporated into the model. Then, the purpose of this paper will be to compare the predicted moisture content and temperature values to the experimental data.

## 2. Mathematical model

A model based on a previous study carried out by Wang and Brennan (1995) was developed in order to simulate the temperature and moisture content within the food.

The main assumptions are: heat and mass transfers are one-dimensional, the transfer in liquid phase is only taken into account, thermophysical properties are supposed to be functions of the moisture content or the temperature, the shrinkage is not considered and the product is viewed as infinite slab.

According to the Fick's second law, the mass conservation equation describing the moisture transfer in the product is:

$$\frac{\partial M}{\partial t} = D_{eff} \frac{\partial^2 M}{\partial x^2} \quad (1)$$

where  $M$  is the moisture content in dry basis (w/w) ( $\text{kg kg}^{-1}$ ),  $t$  is the time (s),  $x$  is the characteristic dimension of the product (m) and  $D_{eff}$  is the effective moisture diffusivity ( $\text{m}^2 \text{s}^{-1}$ ).

Following on from the Fourier's law, the heat conservation equation illustrating the heat transfer in the product is:

$$\rho_p C_p \frac{\partial T}{\partial t} = \lambda_p \frac{\partial^2 T}{\partial x^2} \quad (2)$$

where  $T$  is the temperature ( $^{\circ}\text{C}$ ),  $\rho_p$  is the density ( $\text{kg m}^{-3}$ ),  $C_p$  is the specific heat capacity ( $\text{J kg}^{-1} \text{ }^{\circ}\text{C}^{-1}$ ) and  $\lambda_p$  is the thermal conductivity ( $\text{W m}^{-1} \text{ }^{\circ}\text{C}^{-1}$ ).

The boundary condition at  $x = L$  (upper surface of the product) for Eq(1) states that the liquid water that reaches the upper product surface is immediately vaporized and swept away by the airflow, with  $L$  the thickness of the sample:

$$k_m (C_{surface} - C_{air}) = D_{eff} \frac{\partial M}{\partial x} \quad (3)$$

where  $k_m$  is the mass transfer coefficient ( $\text{m s}^{-1}$ ),  $C_{surface}$  is the water vapor concentration at the product surface ( $\text{kg m}^{-3}$ ) and  $C_{air}$  the water vapor concentration in the air ( $\text{kg m}^{-3}$ ).

In the same way, the boundary condition at  $x = L$  (surface) for Eq(2) is written as:

$$h(T_{air} - T_{surface}) = L_v D_{eff} \frac{\partial M}{\partial x} - \lambda_p \frac{\partial T}{\partial x} \quad (4)$$

where  $h$  is the heat transfer coefficient ( $\text{W m}^{-2} \text{ }^{\circ}\text{C}^{-1}$ ),  $T_{air}$  is the air temperature ( $^{\circ}\text{C}$ ),  $T_{surface}$  is the temperature at the product surface ( $^{\circ}\text{C}$ ) and  $L_v$  is the latent heat of vaporation of water ( $\text{J kg}^{-1}$ ). The term  $L_v D_{eff} \frac{\partial M}{\partial x}$  represents the quantity of heat needed to vaporize the liquid water available at the surface.

The boundaries conditions at  $x = 0$  (bottom surface of the product) for Eq(1) and Eq(2) suppose that no mass and heat is transferred through the bottom product surface:

$$\frac{\partial M}{\partial x} = 0 \text{ and } \frac{\partial T}{\partial x} = 0 \quad (5)$$

## 3. Materials and methods

### 3.1 Samples

A gel made of carboxymethylcellulose (CMC) known as Tylose<sup>®</sup> (purchased at Cuistoshop, Conflans Sainte Honorine, France) was chosen to simulate water-rich foods. This gel was formulated by mixing distilled water and Tylose<sup>®</sup> powder to obtain an initial moisture content of  $(79.1 \pm 0.1) \%$  in wet basis (w/w); corresponding to  $(3.8 \pm 0.1) \text{ kg kg}^{-1}$  in dry basis (w/w). The preparation was carried out according to the protocol published by Anderson and Singh (2005). The initial apparent density of the Tylose<sup>®</sup> gel was measured and is equal to  $1089 \text{ kg m}^{-3}$ .

### 3.2 Desorption isotherms

The calculation of the boundary condition (surface) for Eq(1) requires the knowledge of the desorption isotherms. These data were determined using a climatic chamber (KBF 115, Binder, Wevelgem, Germany) at  $40 \text{ }^{\circ}\text{C}$  and  $70 \text{ }^{\circ}\text{C}$  on a humidity range from  $95 \%$  to  $5 \%$ . For each temperature, three samples of about  $70 \text{ g}$  were weighted using a precision balance (ACCULAB ALC-110.4, accuracy  $\pm 1.10^{-4} \text{ g}$ , Sartorius, Goettingen, Germany) until the equilibrium with the surrounding air was reached (constant mass). Figure 1 presents the

average values determined and the best-fit curves using the GAB model (Eq(6)). A low influence of the temperature was noticed. The Tylose<sup>®</sup> gel is a macroporous product as most of food products.

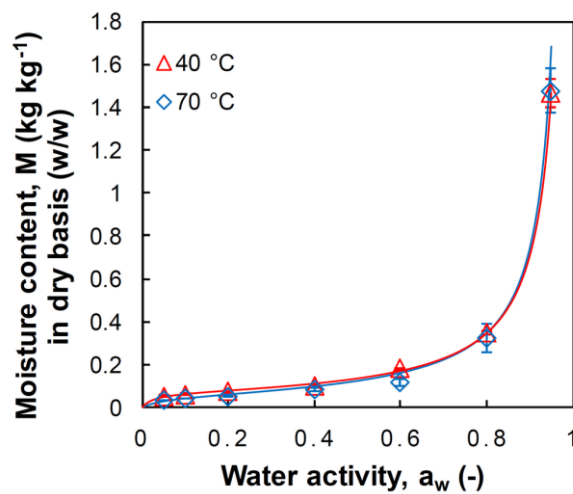


Figure 1: Desorption isotherms for the Tylose<sup>®</sup> gel at 40 °C and 70 °C

The equation and the predicted values by the GAB model are presented in Table 1. No data was published at these temperatures to compare the results.

Table 1: Equations and predicted values by the GAB model

Equation	$M = \frac{M_0 C_g a_w K}{(1 - K a_w)(1 - K a_w + C_g K a_w)}$ (6)					
Temperature (°C)	40			70		
Predicted values	$M_0$	$C_g$	$K$	$M_0$	$C_g$	$K$
	0.07	37	1.00	0.07	15	1.00
Model parameters	$M_0$ : monolayer moisture content (kg kg <sup>-1</sup> ) in dry basis (w/w) $C_g$ : Guggenheim constant (-) $K$ : Factor correcting which takes account the sorption properties of multilayers (-) $a_w$ : Water activity (-)					

### 3.3 Thermal conductivity

The thermal conductivity was needed to calculate Eq(2) and the boundary condition (surface) for Eq(2). Empirical correlations showing the evolution of the thermal conductivity of food components (carbohydrate and water) versus the temperature were evaluated (ASHRAE, 2002).

### 3.4 Heat capacity

The specific heat capacity of the Tylose<sup>®</sup> gel was essential in Eq(2). A mixing law describes the evolution of the specific heat capacity between the specific heat capacity of the pure water and that of the dry solid:

$$c_p(M) = \frac{c_{pd} + M c_{pw}}{1 + M} \quad (7)$$

where  $c_{pw}$  is the specific heat capacity of pure liquid water (J kg<sup>-1</sup> °C<sup>-1</sup>) and  $c_{pd}$  the specific heat capacity of dry matter (J kg<sup>-1</sup> °C<sup>-1</sup>). A microcalorimeter ( $\mu$ DSC3, Setaram, Caluire, France) was used to measure the heat capacity on dry samples in a temperature range of 30 – 90 °C for a sample mass of 300 mg. From these measurements, the dry matter heat capacity was expressed as a linear function of the temperature:

$$c_{pd} = 5.92 \cdot T + 1199 \quad (T \text{ in } ^\circ\text{C}).$$

### 3.5 Air impingement drying

A prototype of an air impingement dryer designed by CIMS (Sablé-sur-Sarthe, France) was used (Figure 2a). The air was directed downwards, from the upper surface towards the inside of the material. To perform jets, a rig composed of triangular nozzles punched of rectangular slots were used (Figure 2b and c). The experimental trials were done at two temperatures (40 °C and 70 °C) and three air velocities (1, 7 and 17 m s<sup>-1</sup>).

Air velocities were measured at the slots outlet using a hot wire anemometer (range 0-50 m s<sup>-1</sup>, accuracy ± 0.01 m s<sup>-1</sup>, TSI, La Garenne-Colombes, France).

Product temperature at the upper surface was measured by type T thermocouple (diameter 0.5 mm, accuracy ± 0.2 °C). Heat flux was measured by a plane fluxmeter (10 × 10 mm, Captec, France) disposed at the upper surface of the product. Five samples were simultaneously dried (dimensions, Figure 2d). Heat flux was obtained by the sample placed in the middle of the tray while the mass loss during the drying was evaluated from the other four samples (Figure 2c).

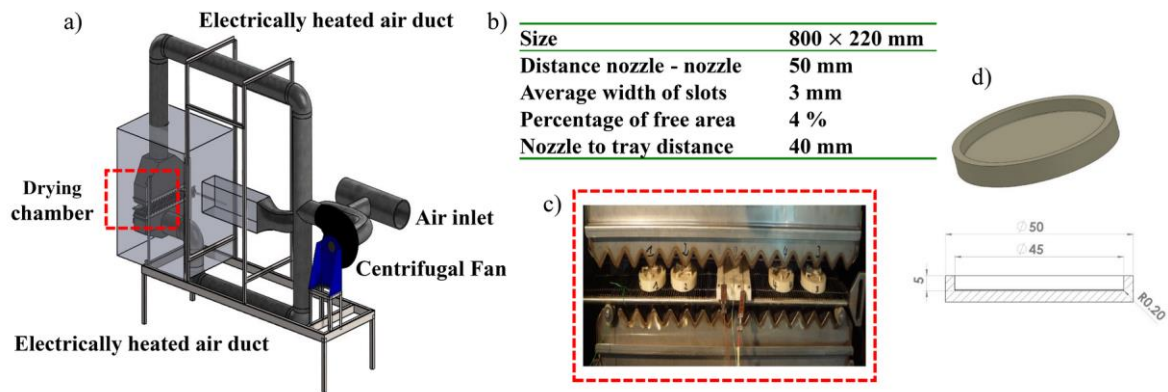


Figure 2: Experimental apparatus a) Schematic diagram of the air impingement jets dryer; b) Design parameters of jets; c) Zoom on air jets setup; d) Shape and dimensions of the samples (in mm)

## 4. Results and discussion

First, an experimental study was carried out to identify the effective moisture diffusivity,  $D_{eff}$ , and the heat transfer coefficient,  $h$ . Then, the model will be experimentally validated by comparison between simulation and measure.

### 4.1 Effective moisture diffusivity

The calculated effective moisture diffusivity is present in the Eq(1) and in the boundaries conditions, i.e. Eq(3) and Eq(4). In our case, the Fick's second law is usable to evaluate the diffusivity since the shrinkage is not taken into account. The procedure to determine  $D_{eff}$  was described in a previous paper (Zaknourne et al., 2013).

The diffusivity increases with the air velocity before stabilizing at about  $2.5 \cdot 10^{-9} \text{ m}^2 \text{ s}^{-1}$  at 40 °C,  $3.5 \cdot 10^{-9} \text{ m}^2 \text{ s}^{-1}$  at 55 °C and  $4.0 \cdot 10^{-9} \text{ m}^2 \text{ s}^{-1}$  at 70 °C from a velocity of 7 m s<sup>-1</sup> (Figure 3a). Beyond this value, the variation of  $D_{eff}$  versus the air velocity is insignificant (deviation less than 10 %). This apparent evolution of the effective diffusivity is related to a non-negligible influence of the external heat transfer coefficient,  $h$ . Then,  $D_{eff}$  should be called apparent effective moisture diffusivity ( $D'_{eff}$ ). As awaited,  $D'_{eff}$  rises significantly with the temperature. Similar tendencies were observed during the convective drying of potato from 40 °C to 85 °C at 0.5 m s<sup>-1</sup> and 1 m s<sup>-1</sup> (Hassini et al., 2007).

The evolution of the apparent effective moisture diffusivity versus the temperature is represented by an Arrhenius equation (Figure 3b).

For the current study, the activation energy,  $E_a$ , is of 17.4 kJ mol<sup>-1</sup> and the pre-exponential factor is equal to  $1.9 \cdot 10^{-6} \text{ m}^2 \text{ s}^{-1}$ . Anderson and Singh (2005) determine apparent effective moisture diffusivities of the Tylose® gel dried in a desiccator:  $4.29 \cdot 10^{-11} \text{ m}^2 \text{ s}^{-1}$  at 2.5 °C,  $7.69 \cdot 10^{-11} \text{ m}^2 \text{ s}^{-1}$  at 7.5 °C and  $9.29 \cdot 10^{-11} \text{ m}^2 \text{ s}^{-1}$  at 12 °C. These values are in accordance with those identified here since a  $R^2$  value of 0.954 was found for the Arrhenius plot combining both studies (Figure 3b).

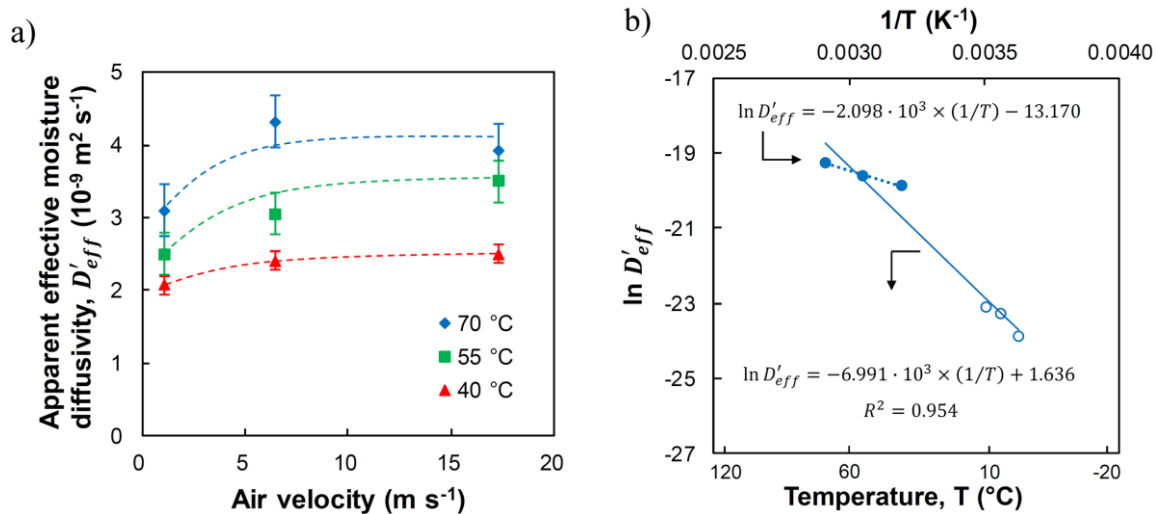


Figure 3: a) Apparent effective moisture diffusivity,  $D'_{eff}$ , versus the air velocity at three temperatures (40, 55 and 70 °C); b)  $\ln D'_{eff}$  versus  $1/T$ . Full symbols: current study and empty symbols: given by Anderson and Singh (2005)

#### 4.2 Heat transfer coefficient

This coefficient was directly measured by recording the heat flux exchanged and the temperature both at the upper surface of the product. The measurement protocol was detailed by Amarante et al. (2003). Similarly, the values of  $h$  measured by the fluxmeter were compared to experimental tests performed with an aluminium plate ( $30 \times 30 \text{ mm}$ ). The lumped capacitance method, was depicted in detail by Mohamed (2008). The correspondent values of heat transfer coefficients are reported in Table 2 as a function of the air velocity at 70 °C.

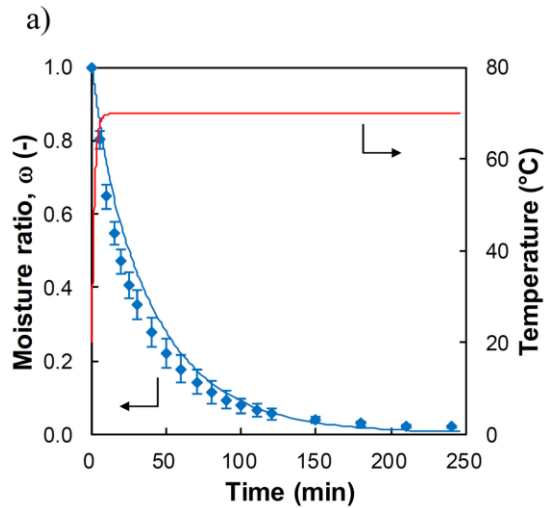
Table 2: Heat transfer coefficients,  $h$ , measured using a fluxmeter and using the lumped capacitance method as a function of the air velocity at 70 °C

Air velocity ( $\text{m s}^{-1}$ )	Fluxmeter $h$ ( $\text{W m}^{-2} \text{ °C}^{-1}$ )	Lumped method $h$ ( $\text{W m}^{-2} \text{ °C}^{-1}$ )	$\Delta h$ ( $\text{W m}^{-2} \text{ °C}^{-1}$ )	$\Delta h/h$ (%)
1	192	135	57	30
7	236	172	36	27
17	245	244	1	0.4

The values measured using a fluxmeter are higher than those obtained from the aluminium plate (Table 2). Amarante et al. (2003) reported the same observation, not for an impingement system, in a lesser extent due to the low velocities applied (from 1 to 7  $\text{m s}^{-1}$ ). Caixeta et al. (2002) reported lower values of  $h$  comprised between  $100 \text{ W m}^{-2} \text{ °C}^{-1}$  and  $160 \text{ W m}^{-2} \text{ °C}^{-1}$  for the impingement drying of potato chips. However, both the method of determination of the heat transfer coefficient and air velocities are not presented.

#### 4.3 Model validation

An experiment (air velocity of 7  $\text{m s}^{-1}$  and temperature of 70 °C) was performed to compare the simulated results with experimental data. For this purpose, both average moisture ratio and temperature at the center of the product were plotted versus time (Figure 4a). The 1D grid was composed of 200 elements disposed in a 5 mm thick domain. Besides, the model accuracy was evaluated through four statistical dimensionless parameters, namely the coefficient of determination ( $R^2$ ), the chi-square ( $\chi^2$ ), the root-mean-square error ( $RMSE$ ) and the residual sum of squares ( $RSS$ ). These parameters were calculated from Eq(8) to Eq(11) summarized in Figure 4b. Simulated results fit the experimental data fairly well (Figure 4b, Eq(8) to Eq(11)). From the drying kinetics, the time needed to reach a residual moisture content of  $0.11 \text{ kg kg}^{-1}$  in dry basis (w/w) is of 4 h. Moreover, it may be noted that the corresponding water activity value is of 0.45 (Figure 1).



b)

$$R^2 = 1 - \frac{\sum_{i=1}^N (\omega_{sim,i} - \omega_{exp,i})^2}{\sum_{i=1}^N (\omega_{exp,i} - \bar{\omega}_{exp,i})^2} = 0.994 \quad (8)$$

$$\chi^2 = \frac{\sum_{i=1}^N (\omega_{exp,i} - \omega_{sim,i})^2}{N - p} = 4.758 \cdot 10^{-4} \quad (9)$$

$$RMSE = \frac{1}{N} \cdot \sqrt{\sum_{i=1}^N (\omega_{sim,i} - \omega_{exp,i})^2} = 0.021 \quad (10)$$

$$RSS = \sum_{i=1}^N (\omega_{exp,i} - \omega_{sim,i})^2 = 0.009 \quad (11)$$

Figure 4: a) Comparison between simulated (full lines) and experimental results (symbols) for  $7 \text{ m s}^{-1}$  at  $70 \text{ }^\circ\text{C}$ ; b) Evaluation of the model's accuracy: statistical analysis of the data (dimensionless values)

## 5. Conclusions

This work was focused on the development of heat and mass transfer model able to predict temperature and moisture content fields in food products during air impingement jets drying. The numerical model was experimentally validated.

## Acknowledgments

The authors would like to thank the French Regional Council of Brittany (SECALIN project grant no. 0311/16007866/00000538) and CIMS for their support.

## References

- Amarante A., Lanoisellé J.-L., Ramirez A., 2003, Direct measurement of heat transfer rates and coefficients in freezing processes by the use of heat flux sensors, *Chemical Engineering Research and Design*, 81, 1105-1112.
- Anderson B.A., Singh R.P., 2005, Moisture Diffusivity in Tylose Gel (Karlsruhe Test Material), *Journal of Food Science*, 70, 331-337.
- ASHRAE (Ed), 2002, 2002 ASHRAE Handbook: Refrigeration, Atlanta, USA.
- Caixeta A.T., Moreira R., Castell-Perez M.E., 2001, Impingement drying of potato chips, *Journal of Food Process Engineering*, 25, 63-90.
- Cascone G., Setegn H.G., Miccio M., Diaferia C., 2015, A tool for modelling and simulation of irregular shape and shrinking salami during drying, *Chemical Engineering Transactions*, 43, 103-108.
- Erbay Z., Icier F., 2010, A review of thin layer drying of foods: Theory, modeling, and experimental results, *Critical Reviews in Food Science and Nutrition*, 50, 441-464.
- Hassini L., Azzouz S., Peczkalski R., Belghith A., 2007, Estimation of potato moisture diffusivity from convective drying kinetics with correction for shrinkage, *Journal of Food Engineering*, 79, 47-56.
- Mohamed, I.O., 2008, An inverse lumped capacitance method for determination of heat transfer coefficients for industrial air blast chillers, *Food Research International*, 41, 404-410.
- Mujumdar A.S. (Ed), 2006, *Handbook of industrial drying*, CRC Press Taylor & Francis Group, Boca Raton, USA.
- Reyes A., Mahn A., Cares V., 2015, Analysis of dried onions in a hybrid solar dryer, freeze dryer and tunnel dryer, *Chemical Engineering Transactions*, 43, 139-144.
- Wang N., Brennan J.G., 1995, A mathematical model of simultaneous heat and moisture transfer during drying of potato, *Journal of Food Engineering*, 24, 47-60.
- Zakoune A., Glouannec P., Salagnac P., 2013, Identification of the liquid and vapour transport parameters of an ecological building material in its early stages, *Transport in Porous Media*, 98, 589-613.